

Unambiguous observation of shape effects on cellular fate of nanoparticles

Zhiqin Chu¹, Silu Zhang¹, Bokai Zhang¹, Chunyuan Zhang², Chia-Yi Fang³, Ivan Rehor⁴, Petr Cigler⁴, Huan-Cheng Chang³, Ge Lin², Renbao Liu¹, Quan Li^{1,*}

1. Department of Physics and Centre for Quantum Coherence, The Chinese University of Hong Kong, Shatin, New Territories, Hong Kong
2. School of Biomedical Sciences, Faculty of medicine, The Chinese University of Hong Kong, Shatin, New Territories, Hong Kong
3. Institute of Atomic and Molecular Sciences, Academia Sinica, Taipei 106, Taiwan
4. Laboratory of Synthetic Nanochemistry, Institute of Organic Chemistry and Biochemistry AS CR, v.v.i., Flemingovo nam. 2, 166 10, Prague 6, Czech Republic

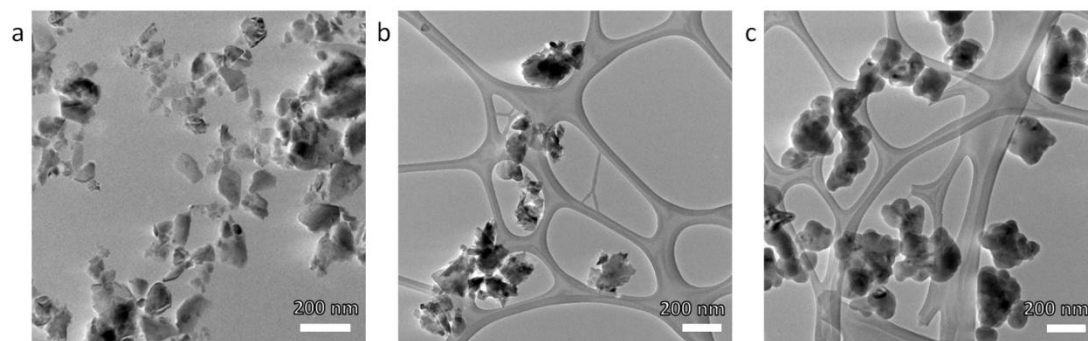
Supplementary Text

Cellular uptake of NDs was shown by confocal microscopy images taken from HepG2 cells fed with NDs for various durations (3, 12, and 24 hours, see Supplementary Fig. S5). The amount of NDs uptaken by the cells increased with the incubation duration. By pretreating cells with endocytic inhibitor before feeding the NDs, we examined the uptake pathway of the NDs. The NDs took endocytosis as the major route of cellular entry, instead of direct membrane penetration. As shown in Figure S6 in Supplementary Information, prior cellular treatment with NaN_3 or at 4°C (knowing to disturb the formation of ATP and thus blocking endocytosis¹) decreased the cellular uptake of NDs by >80%. This result suggested endocytosis as the major uptake mechanism. Further evidence came from time dependent co-localization investigation of NDs and endosomes (stained by endosome marker), or NDs and lysosomes (stained by lysotracker). With short incubation duration (~1 hour), most of the NDs were found to reside in endosomes (overlap coefficient ~0.8 for 1 hour incubation, as shown in Fig. 2c & 2m), which is a signature of endocytosis.

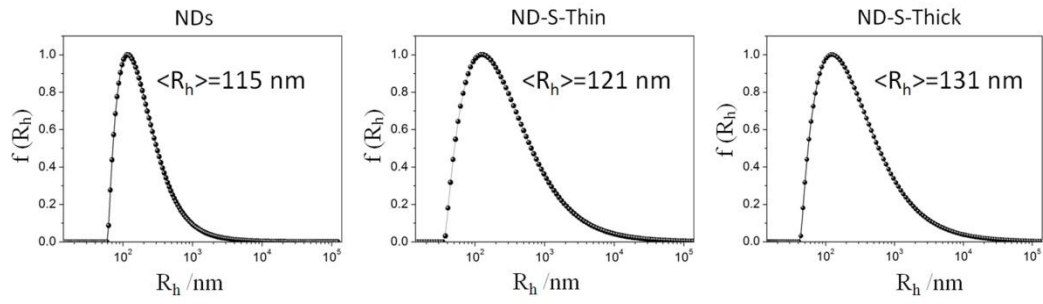
It has been known that the size of NPs plays an important role in their cellular uptake. The works in literature suggest that the amount of NPs that can be internalized is affected by the size of the NPs². An optimum size was proposed for increasing the likelihood of endocytosis due to competition between the thermal dynamic driving force for engulfing and the recruitment kinetics of receptors to the binding site of plasma membrane³. Nevertheless, we found the major cellular uptake route of NPs was not significantly affected by size (for size in the range of tens to hundreds of nanometers in the present study) — the NPs always took endocytosis as the major cellular entry pathway instead of via direct penetration. Similar observations were made when the incubation were carried out in either serum free or serum containing medium, suggesting the minor role of possible protein corona formation on the surface of NDs in determining their intracellular translocation (Fig. S19).

We have carried out the same experiments in other cell lines (common human colon cancer HCT116 cell line and human breast cancer LCC6 cell line), and obtained similar results. The only difference was the time scale of ND's endosomal escape. For HCT116 cells, NDs' escaping from endosomes to cytoplasm was observed when the incubation duration was longer than 1.5 hours (overlap coefficient of NDs with endosome marker gradually decreased from ~0.9 (at 1.5 hours incubation) to ~0.1 (at 4 hours incubation), as shown in Fig. S7 a-k). As a comparison, obvious endosomal release of NDs in the LCC6 cells occurred only when the incubation duration was longer than 2 hours (overlap coefficient of NDs with endosome marker gradually decreased from ~0.8 (2 hours) to ~0.1 (4 hours), as shown in Fig. S8 a-k). For both HCT116 and LCC6 cells, we always found that most NDs only resided in early endosomes, and they seldom had chance to be translocated to late endosomes or lysosomes, before they escaped to the cytoplasm (overlap coefficient of NDs with lysotracker remained at ~0.2 for all time points, as shown in Fig. S7 and S8). These

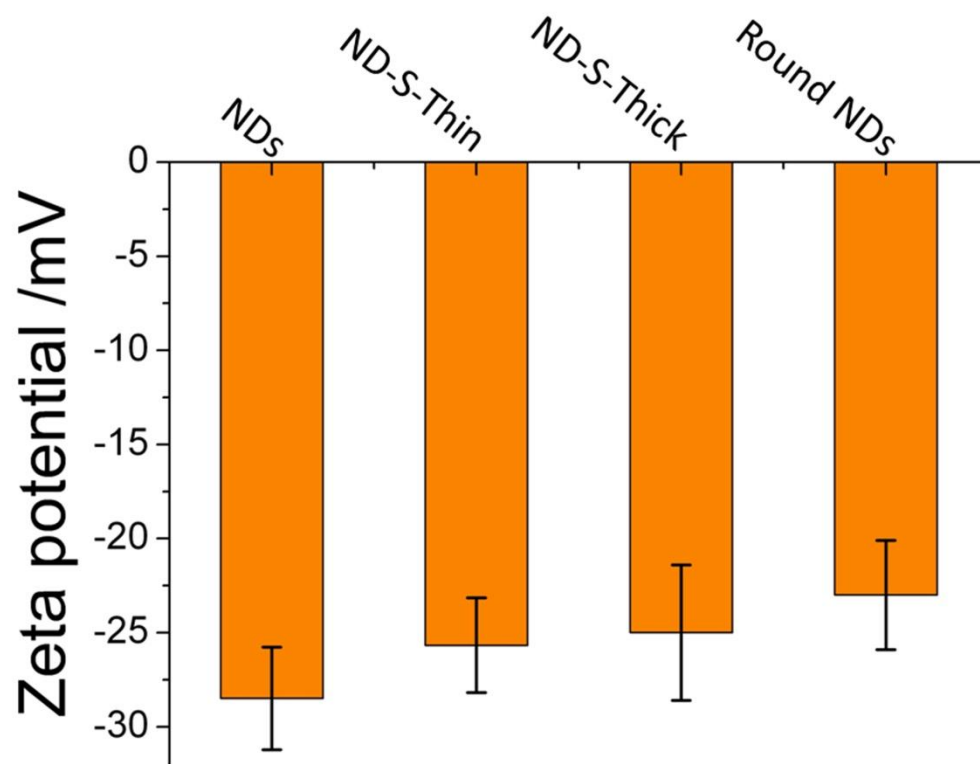
results were further supported by our TEM study, i.e., most of the NDs in either HCT116 (See Fig. S7 n & o) or LCC6 cells (See Fig. S8 n & o) after a longer period of incubation (24 hours) were found in cytoplasm.



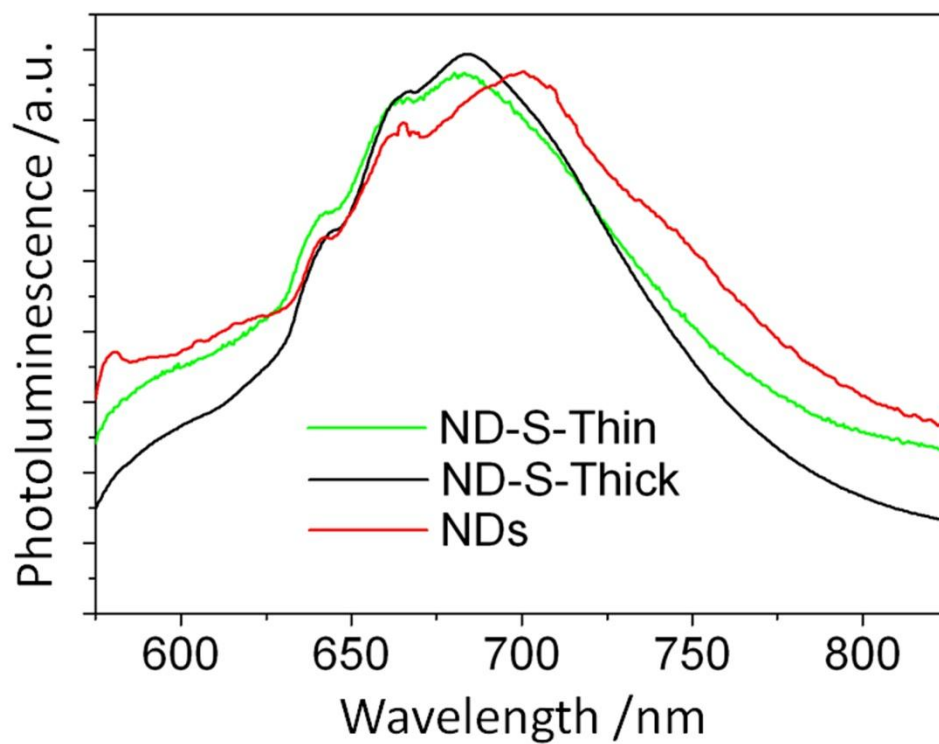
Supplementary Figure S1. Low magnification TEM image of (a) NDs, (b) ND-S-Thin and (c) ND-S-Thick particles.



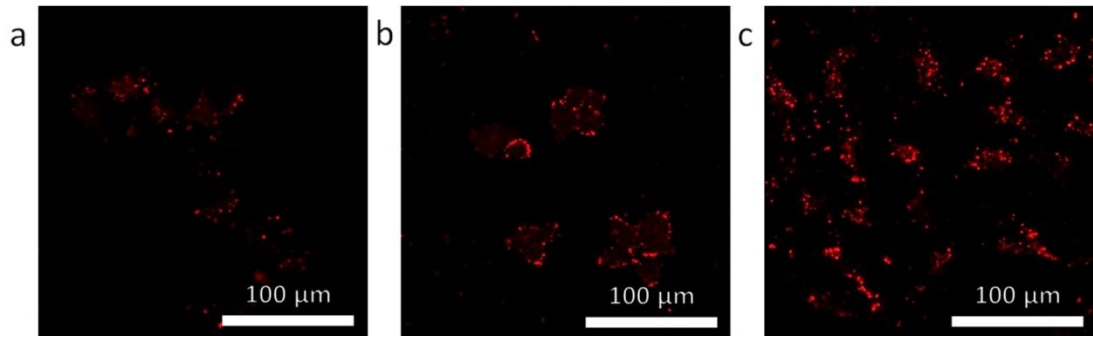
Supplementary Figure S2. Dynamic light scattering results of NDs, ND-S-Thin and ND-S-Thick particles dispersed in PBS buffer at concentration of 10 $\mu\text{g}/\text{ml}$. The hydrodynamic radius of particles is depicted on the horizontal axis and the corresponding frequency on the vertical axis. The insert is the average hydrodynamic radius for each sample revealed by the peak value in the spectra.



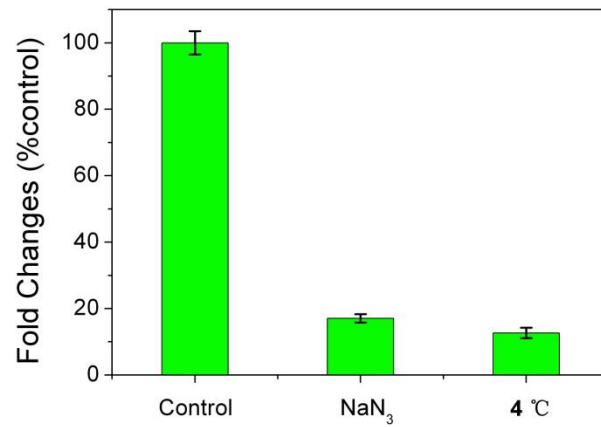
Supplementary Figure S3. Zeta potential of uncoated NDs, ND-S-Thin, ND-S-Thick and Round NDs particles dispersed in PBS buffer.



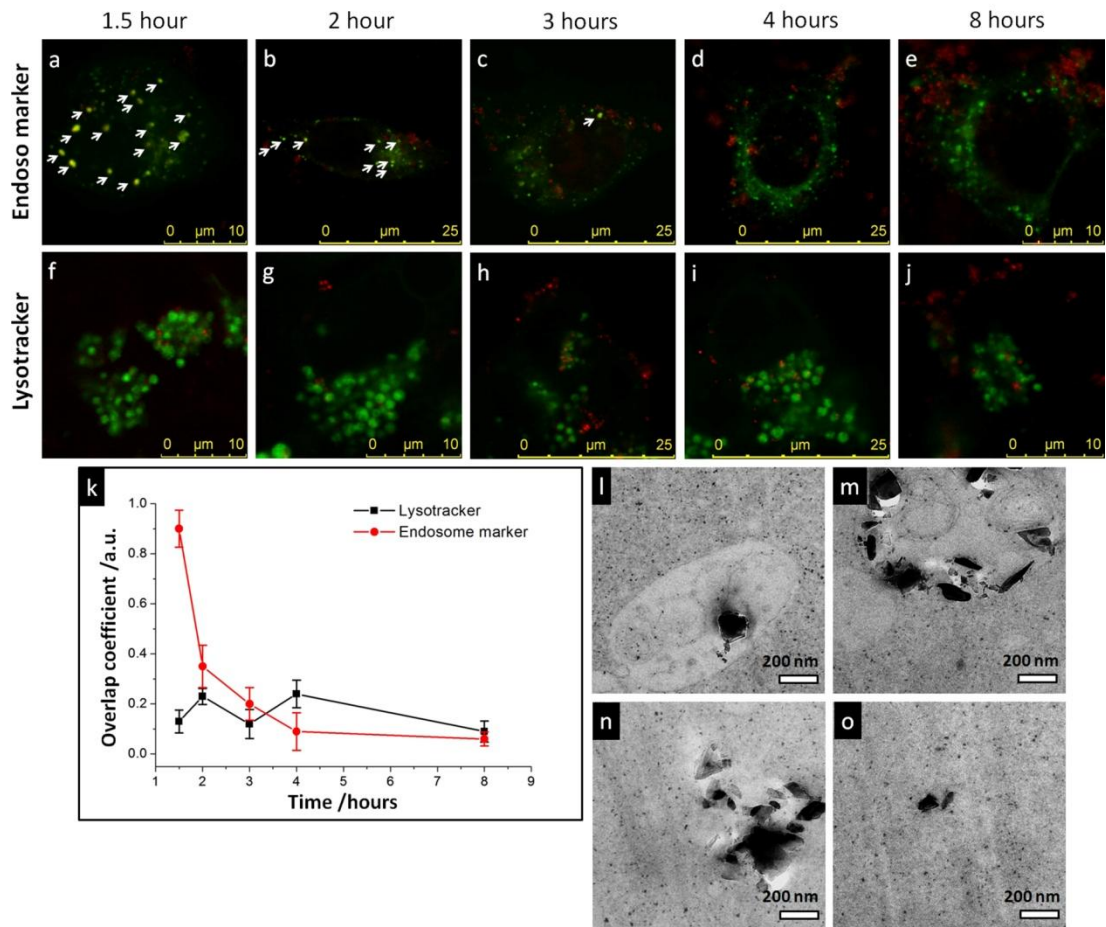
Supplementary Figure S4. Photoluminescence spectra of NDs, ND-S-Thin and ND-S-Thick particles. The wavelength of excitation laser is 514 nm.



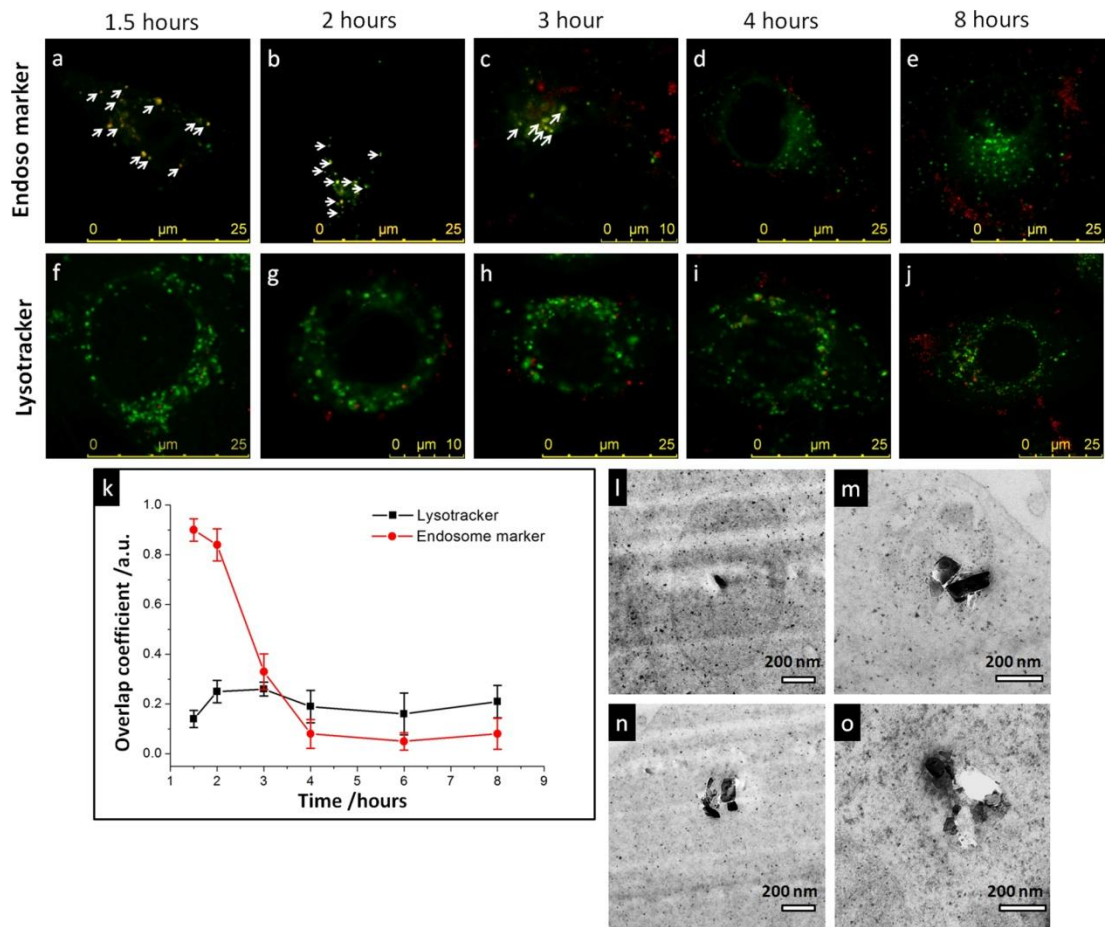
Supplementary Figure S5. Confocal microscopy images of HepG2 cells incubated with NDs for (a) 3, (b) 12 and (c) 24 hours in serum-free medium.



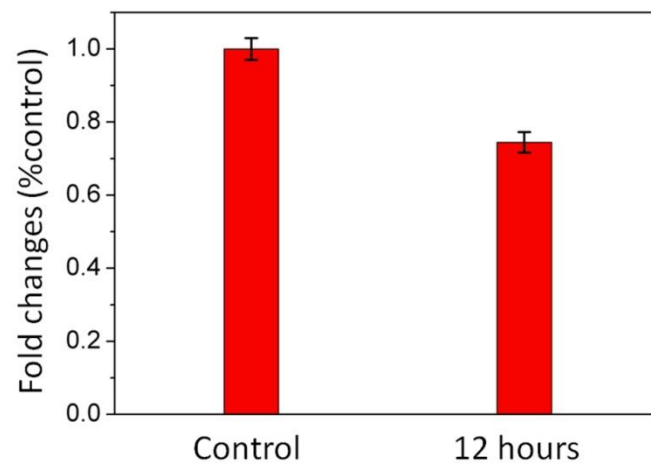
Supplementary Figure S6. Elucidating cellular uptake mechanisms of NDs. Quantitative flow-cytometry data showing the inhibition of NDs' uptake in the presence of 4°C/NaN₃ (blocking the energy-dependent endocytosis). The error bar showed the standard deviation (SD) from three independent experiments. The cells treated with NDs alone were used as the control.



Supplementary Figure S7. Spatiotemporal evolution of NDs inside HCT116 cells. (a-e) Representative confocal microscopy images showing the fluorescent signal of endosome markers (green) and NDs (red) in HCT116 cells after cells incubation with NDs in serum-free medium for (a) 1.5 hours, (b) 2 hours, (c) 3 hours, (d) 4 hours and (e) 8 hours. The yellow spots indicate the co-localization of NDs and endosomes (as marked by white arrows). (f-j) Representative confocal microscopy images showing the fluorescent signal of lysotracker (green) and NDs (red) in HCT116 cells after cells incubation with NDs in serum-free medium for (f) 1.5 hours, (g) 2 hours, (h) 3 hours, (i) 4 hours and (j) 8 hours. (k) The overlap coefficient of NDs with either endosome markers or lysotracker as a function of incubation duration, the error bar showed the standard deviation from 3 different cell samples at each time point. (l-o) TEM images showing the typical distribution of NDs in HCT116 cells after their 24 hours' incubation in serum-free medium: (l) NDs residing in a membrane-bounded vesicle; (m) NDs penetrating the membrane of the vesicle; (n, o) NDs in cytoplasm (majority).

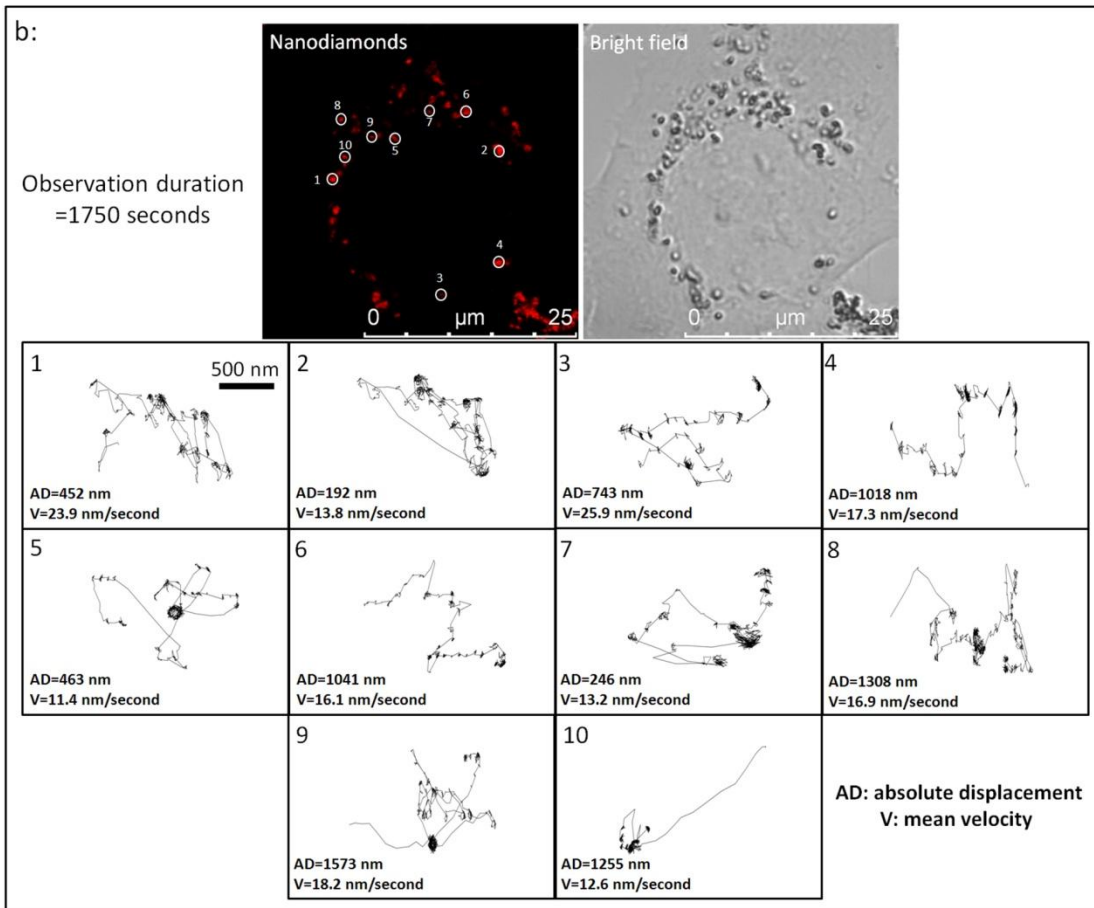
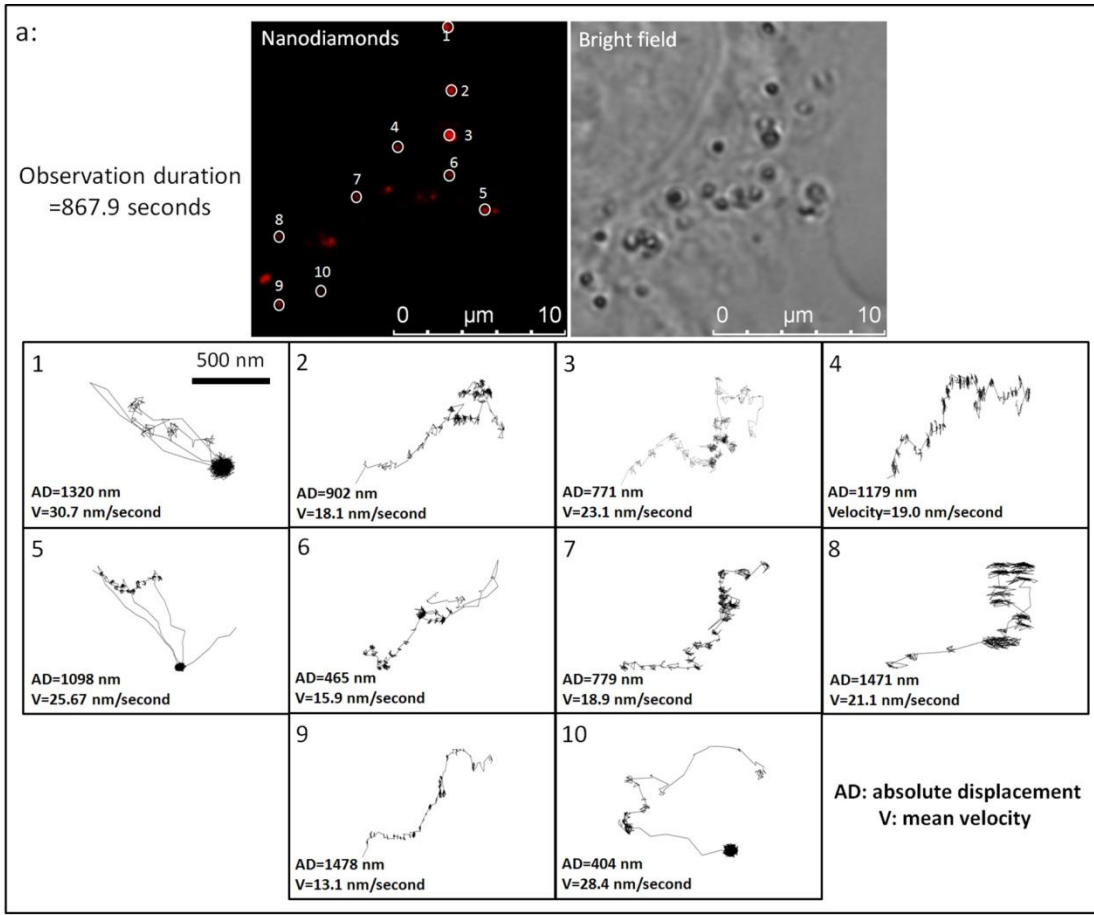


Supplementary Figure S8. Spatiotemporal evolution of NDs inside LCC6 cells. (a-f) Representative confocal microscopy images showing the fluorescent signal of endosome markers (green) and NDs (red) in LCC6 cells after cells incubation with NDs in serum-free medium for (a) 1.5 hours, (b) 2 hours, (c) 3 hours, (d) 4 hours and (e) 8 hours. The yellow spots indicate the co-localization of NDs with endosomes (as marked by white arrows). (f-j) Representative confocal microscopy images showing the fluorescent signal of lysotracker (green) and NDs (red) in LCC6 cells after cells incubation with NDs in serum-free medium for (f) 1.5 hours, (g) 2 hours, (h) 3 hours, (i) 4 hours and (j) 8 hours. (k) The overlap coefficient of NDs with either endosome markers or lysotracker as a function of incubation duration, the error bar showed the standard deviation from 3 different cell samples at each time point. (l-o) TEM images showing the typical distribution of NDs in LCC6 cells after their 24 hours' incubation in serum-free medium: (l) NDs residing in a membrane-bounded vesicle; (m) NDs penetrating the membrane of the vesicle; (n, o) NDs in cytoplasm (majority).

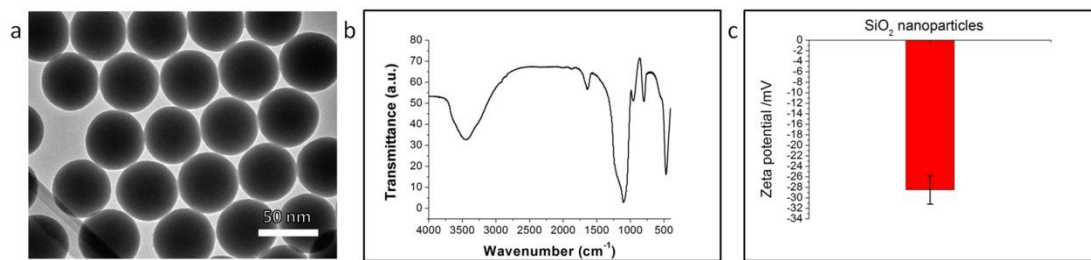


Supplementary Figure S9. Quantitative flow-cytometry data showing the hard excretion of NDs.

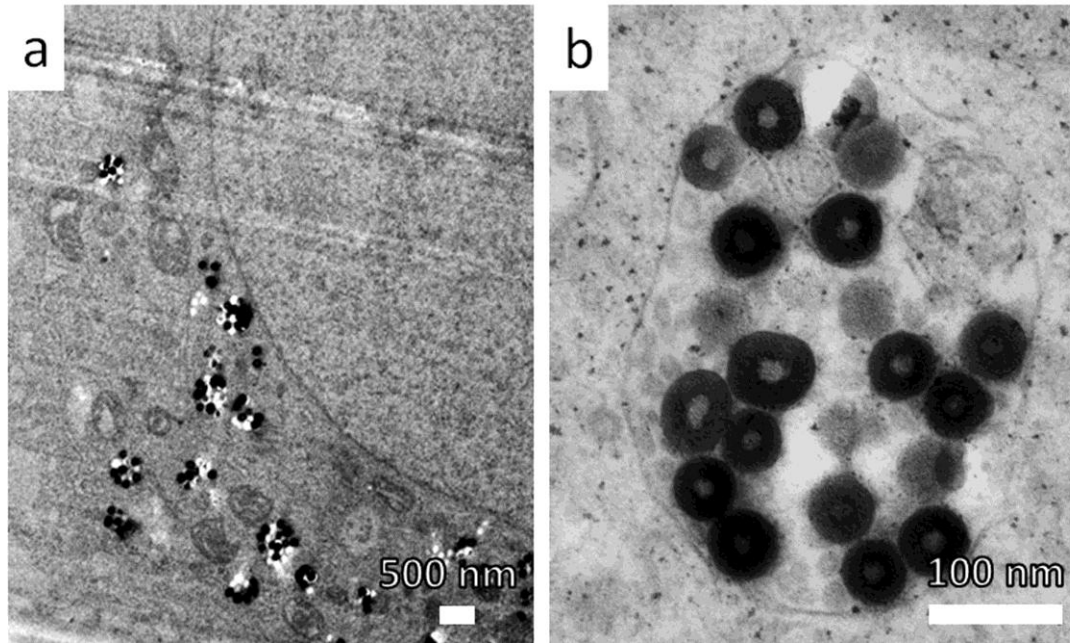
HepG2 cells were incubated with nanodiamonds in serum-free medium for 12 hours (Control), followed by wash and incubated for additional 12 hours in serum-free medium without nanodiamonds (12 hours).



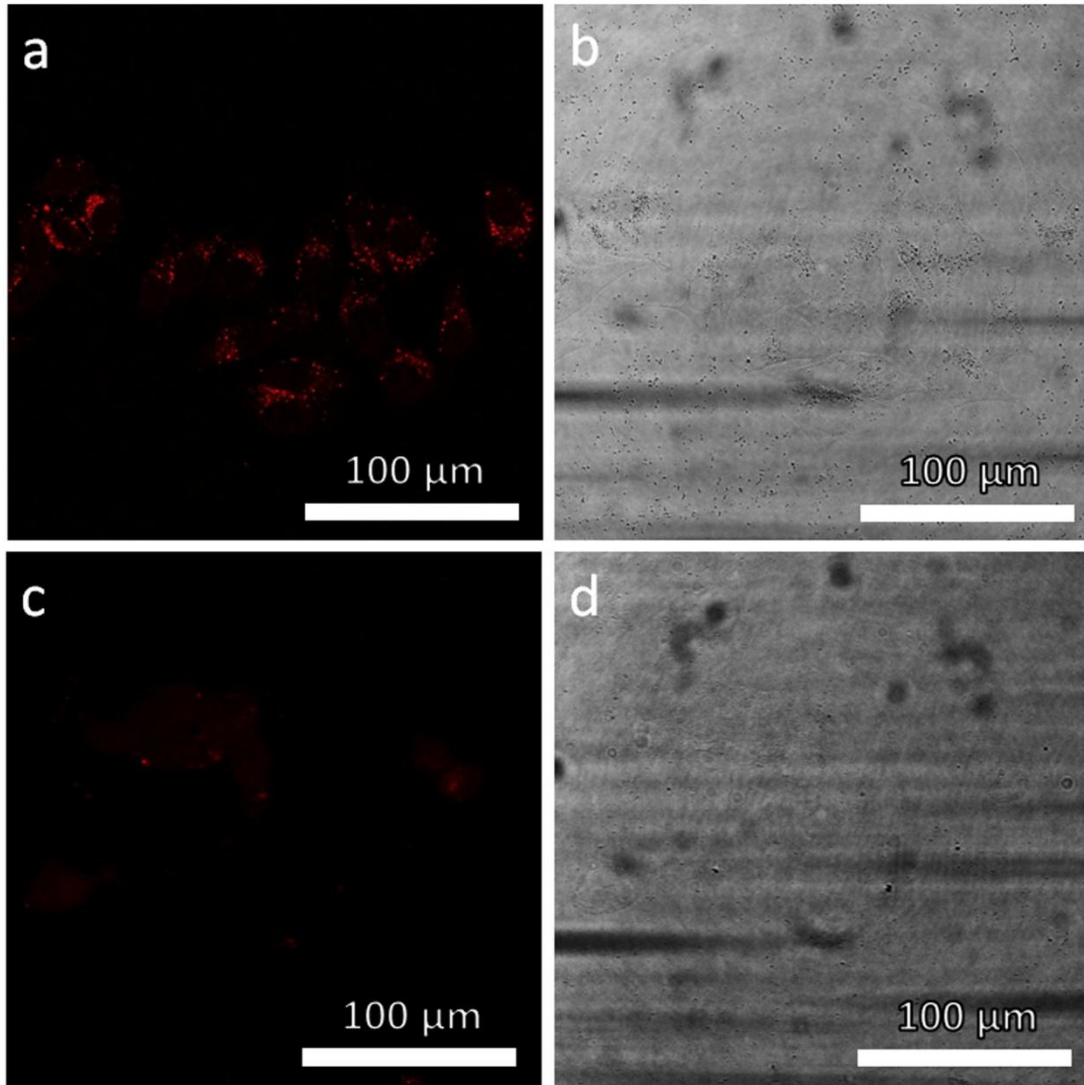
Supplementary Figure S10. Real time multiple particle tracking of the NDs after 24 hours' incubation with HepG2 cells in serum-free medium. (a) 10 randomly chosen NDs and/or NDs aggregates were tracked for 867.9 seconds with a speed of 1.315 second/frame. (b) 10 randomly chosen NDs and/or NDs aggregates were tracked for 1750 seconds with a speed of 2 second/frame. The trajectories, absolute displacement and mean velocity for each group were illustrated in the figures.



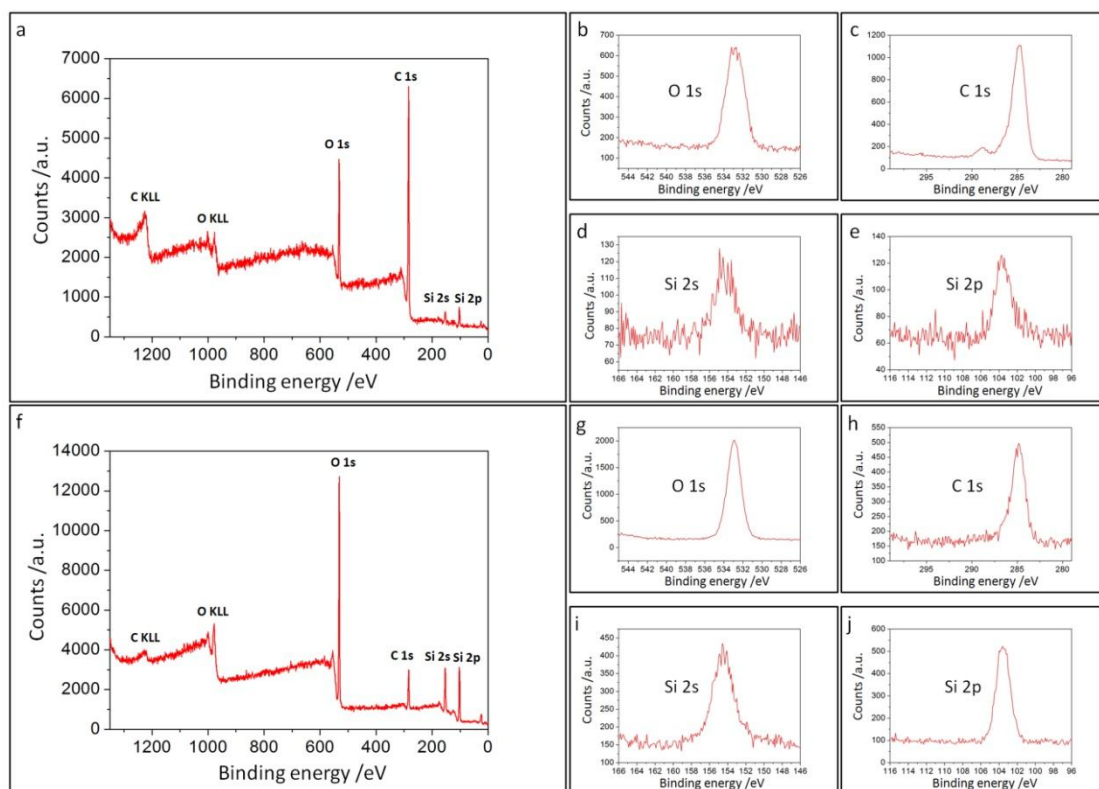
Supplementary Figure S11. Characterizations of SiO₂ NPs. (a) TEM image of SiO₂ NPs (~50 nm in diameter). (b) FTIR spectrum of SiO₂ NPs showing the typical surface chemistry of SiO₂. (c) Zeta potential of SiO₂ NPs in PBS buffer.



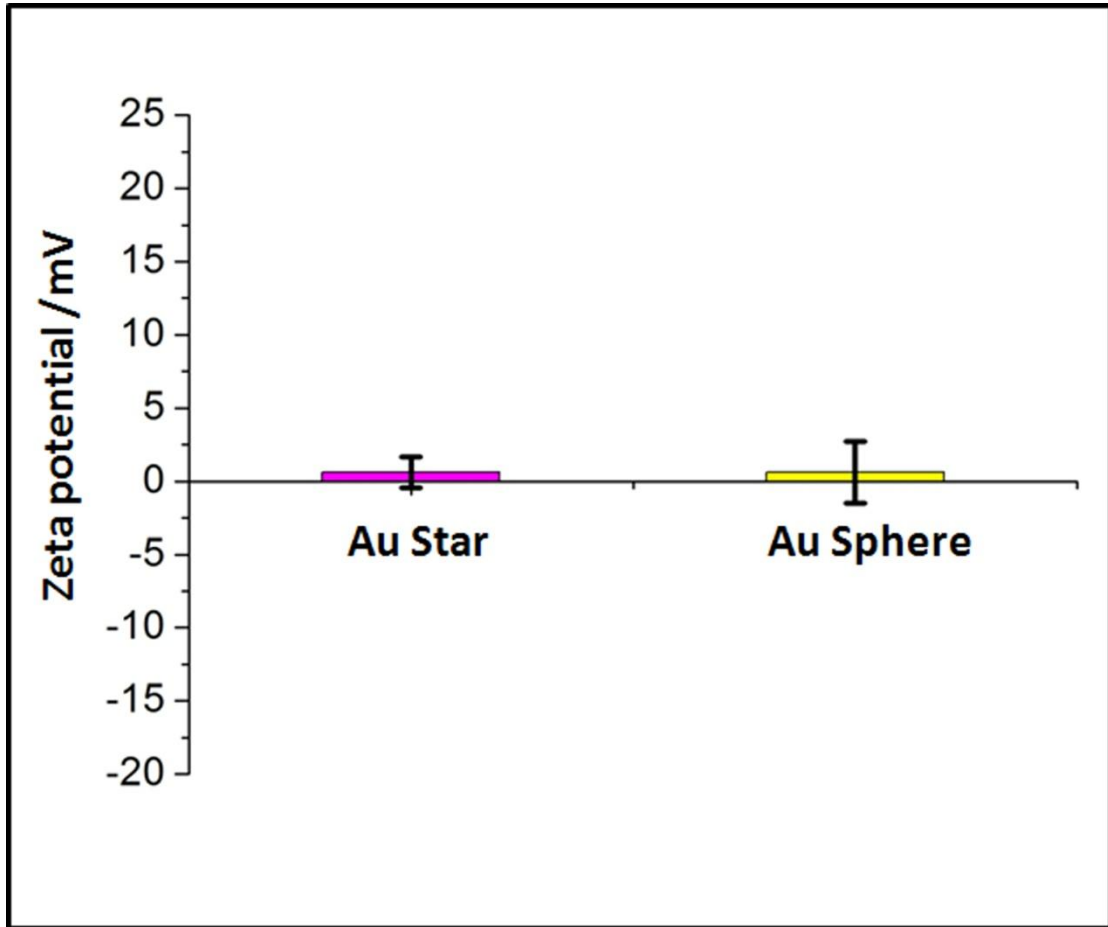
Supplementary Figure S12. TEM images of the HepG2 cells treated with 50 nm SiO₂ NPs. The images were taken from cell samples incubated with the SiO₂ NPs in serum-free medium for 24 hours. (a) TEM image showing the SiO₂ NPs inside a typical cell. (b) Enlarged TEM image showing that the NPs always reside in membrane bounded vesicles.



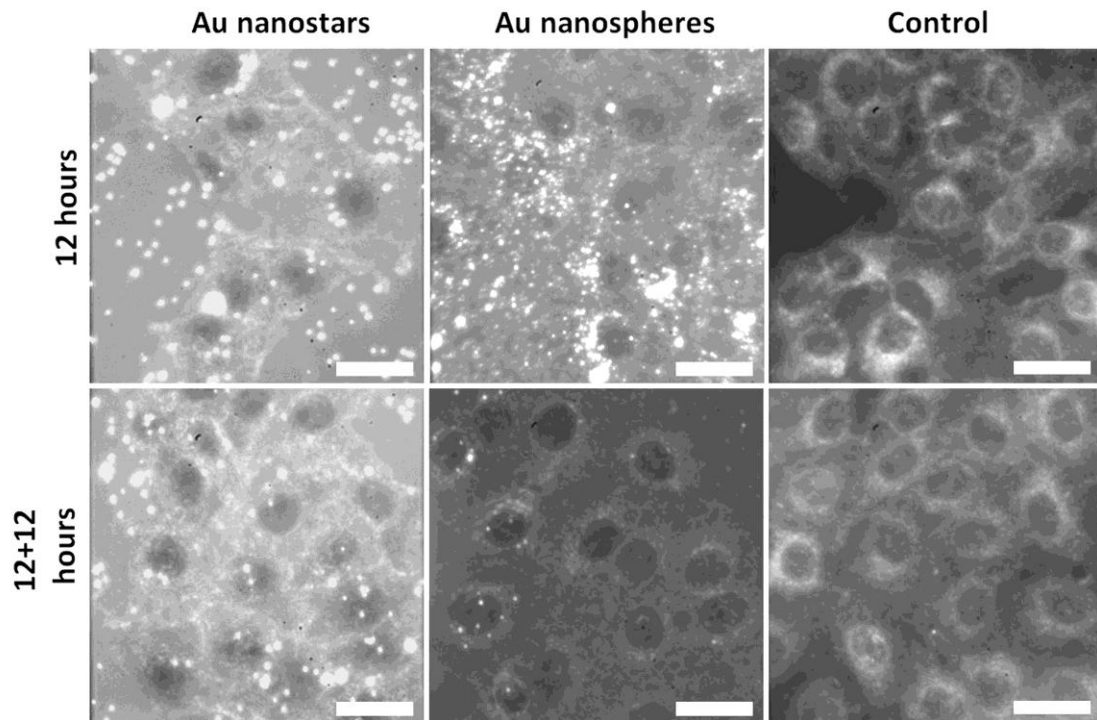
Supplementary Figure S13. Confocal microscopy images of HepG2 cells treated with 50 nm fluorescent amorphous silica NPs. Fluorescence image (a) and transmittance image (b) of HepG2 cells treated with NPs in serum-free medium for 12 hours. Fluorescence image (c) and transmittance image (d) of HepG2 cells after an additional 12 hours incubation in NPs-free serum-free medium.



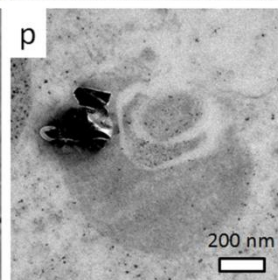
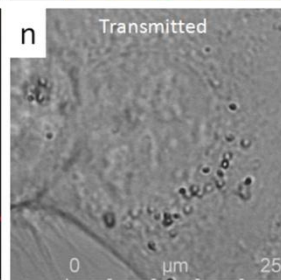
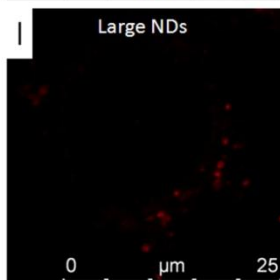
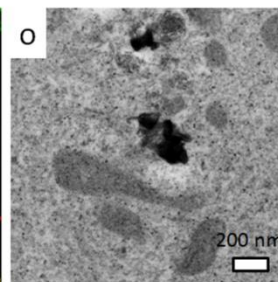
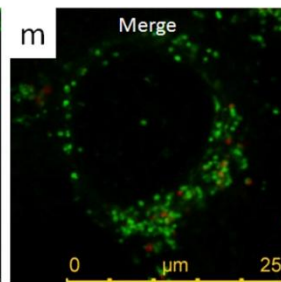
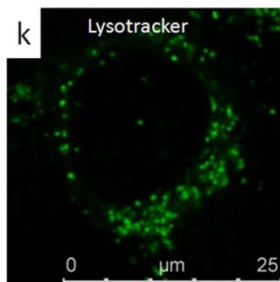
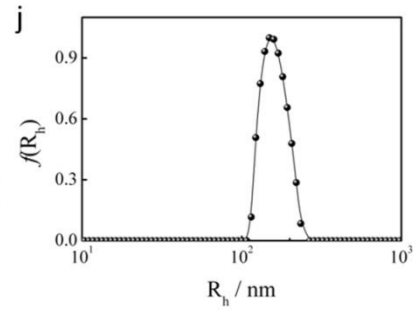
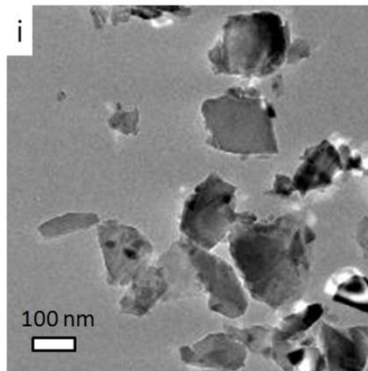
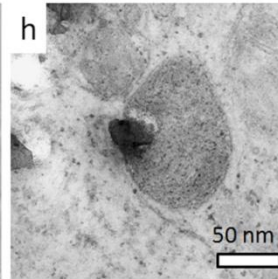
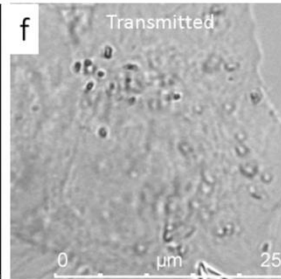
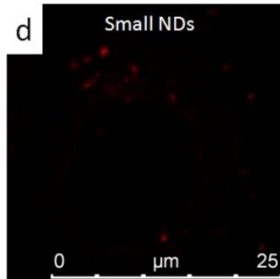
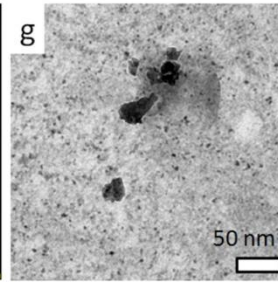
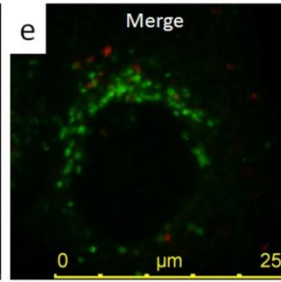
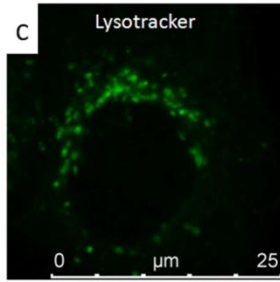
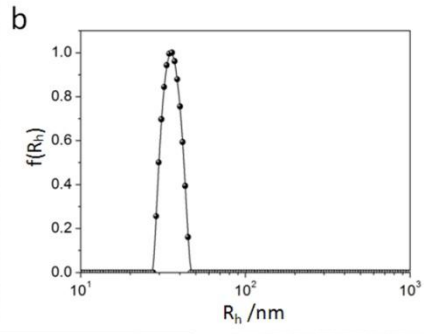
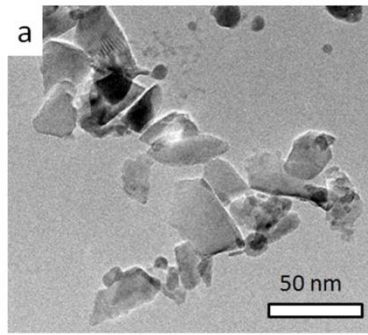
Supplementary Figure S14. Characterizations of ND-S-Thin and ND-S-Thick samples. (a-j) Typical X-ray photoelectron spectroscopy (XPS) spectra taken from ND-S-Thin and ND-S-Thick particles sample. (a-e) XPS spectra taken from ND-S-Thin particles sample: (a) survey scan of ND-S-Thin particles sample, and fine scan of (b) O 1s, (c) C 1s, (d) Si 2s and (e) Si 2p. (f-j) XPS spectra taken from ND-S-Thick particles sample: (f) survey scan of ND-S-Thick particles sample, and fine scan of (g) O 1s, (h) C 1s, (i) Si 2s and (j) Si 2p. The fine scan of Si and O peak revealed that they form SiO_2 , and the C peak characteristic of diamond also presented.



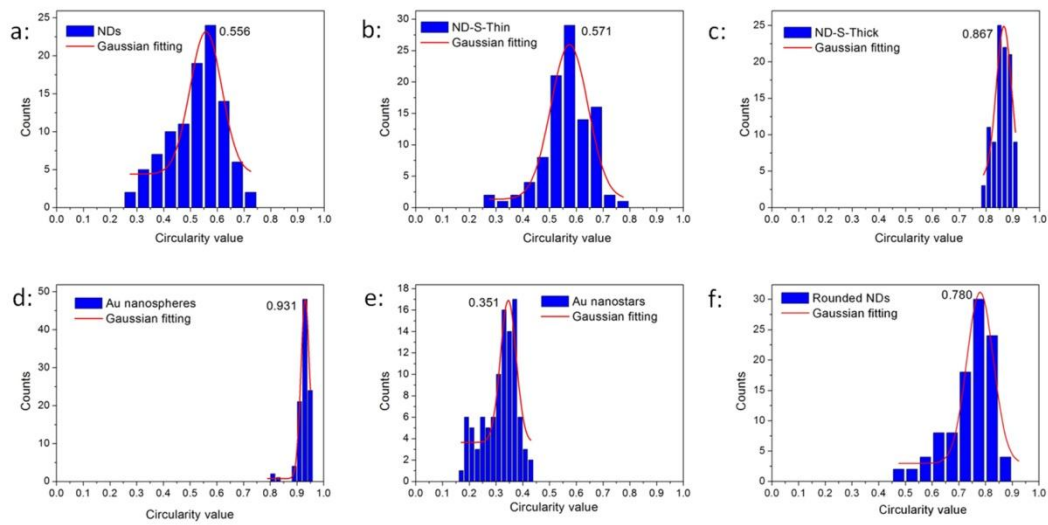
Supplementary Figure S15. Zeta potential of Au nanostars and Au nanospheres in PBS buffer.



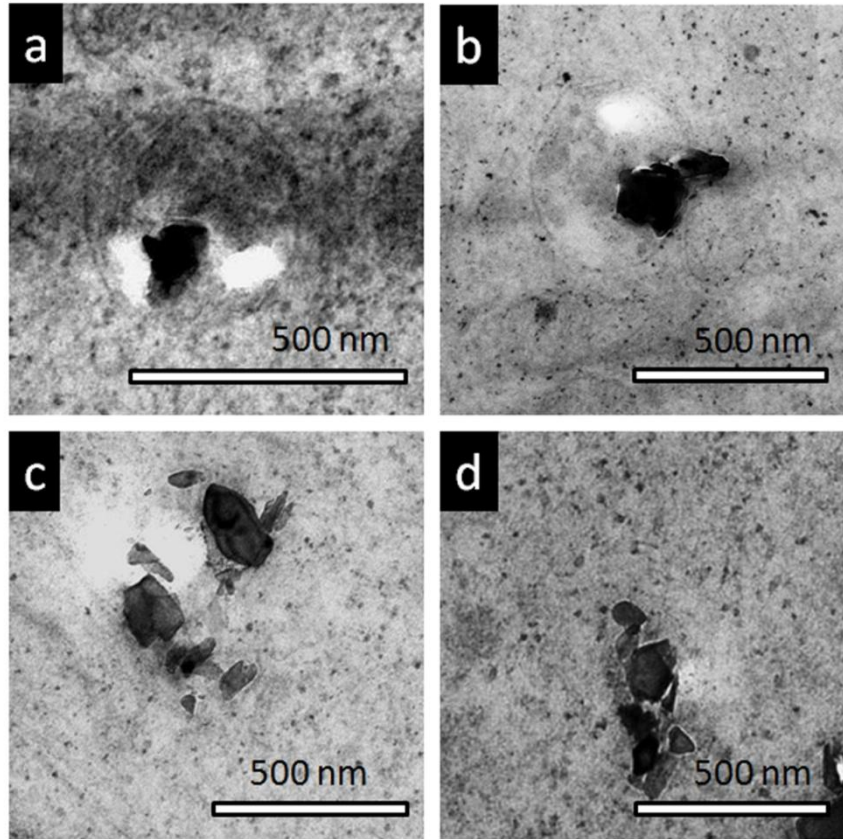
Supplementary Figure S16. Excretion of Au nanostars and Au nanospheres in HepG2 cells were tested using dark field microscopy. The upper row shows the cells incubated with Au nanostars, Au nanospheres in serum-free medium for 12 hours, and the lower row shows the cells incubated with additional 12 hours in NPs-free serum-free medium. The cells treated with NPs-free serum-free medium only were chosen as control. The scale bar is 20 μm .



Supplementary Figure S17. Intracellular translocation of small NDs (~ 35 nm) and large NDs (~150 nm) in HepG2 cells. (a) High-resolution TEM image showing the morphology of small NDs (~35 nm), which was similar to that of the big ones. (b) DLS result of small NDs in PBS buffer at 10 µg/ml. (c-f) Confocal microscopy images showing the colocalization of NDs (~35 nm) with lysotracker in a cell after 24 hours' cell incubation with NDs (~35 nm) in serum-free medium: (c) the fluorescent signal of lysotracker (green); (d) the fluorescent signal of NDs (~35 nm) (red); (e) the overlapping image of (c) and (d), the overlap coefficient was determined as 0.14 by ImageJ; (f) the transmitted light image showing the morphology of the chosen cell. (g,h) TEM images showing the typical intracellular distribution of small NDs (~35 nm) in HepG2 cells after their 24 hours' incubation in serum-free medium: (g) small NDs in cytoplasm; (h) small NDs penetrating the membrane of the vesicle. (i) High-resolution TEM image showing the morphology of large NDs (~150 nm), which was similar to that of the small ones. (l) DLS result of large NDs in PBS buffer at 10 µg/ml. (k-n) Confocal microscopy images showing the colocalization of NDs (~150 nm) with lysotracker in a cell after 24 hours' cell incubation with NDs (~150 nm) in serum-free medium: (k) the fluorescent signal of lysotracker (green); (l) the fluorescent signal of NDs (~150 nm) (red); (m) the overlapping image of (k) and (l), the overlap coefficient was determined as 0.19 by ImageJ; (n) the transmitted light image showing the morphology of the chosen cell. (o,p) TEM images showing the typical intracellular distribution of large NDs (~150 nm) in HepG2 cells after their 24 hours' incubation in serum-free medium: (o) large NDs in cytoplasm; (p) large NDs penetrating the membrane of the vesicle.



Supplementary Figure S18. The distribution of circularity in different NPs. (a) NDs; (b) ND-S-Thin; (c) ND-S-Thick; (d) Au nanospheres; (e) Au nanostars and (f) rounded NDs particles. The circularity was obtained by randomly choosing 100 particles from their High-resolution TEM images for each sample, and then analyzed using ImageJ software.



Supplementary Figure S19. Intracellular distribution of NDs for cells incubated in serum-containing medium. TEM images showing the typical intracellular distribution of NDs in HepG2 cells after their 24 hours' incubation in serum-containing medium: (a) NDs residing in a membrane-bounded vesicle; (b) NDs penetrating the membrane of the vesicle; (c, d) NDs in cytoplasm (majority).

Supplementary Table S1. Relation between sharpness of nanoparticles and their distribution in cytoplasm. The average circularity, defined as $4A\pi/(P^2)$ with A being its area and P its perimeter, describes the sharpness of different types of nanoparticles. The intracellular distribution of various nanoparticles after 24 hours' incubation in serum-free medium were obtained by randomly choosing several tens of cells in >100 TEM images for each sample.

Samples	Prickly NDs	Round NDs	ND-S-Thin	ND-S-Thick	Au nanostars	Au nanospheres
Average circularity	0.556	0.780	0.571	0.867	0.351	0.931
Probability in cytoplasm	~90 %	~10%	~90 %	~10 %	~95 %	~10 %

Reference

- 1 Schmid, S. L. & Carter, L. L. Atp Is Required for Receptor-Mediated Endocytosis in Intact-Cells. *J. Cell Biol.* **111**, 2307-2318 (1990).
- 2 Chithrani, B. D. & Chan, W. C. W. Elucidating the mechanism of cellular uptake and removal of protein-coated gold nanoparticles of different sizes and shapes. *Nano Lett.* **7**, 1542-1550 (2007).
- 3 Zhang, S. L., Li, J., Lykotrafitis, G., Bao, G. & Suresh, S. Size-Dependent Endocytosis of Nanoparticles. *Adv. Mater.* **21**, 419-424 (2009).